

Jamison Assunção Victor Sacek

Department of Geophysics, Universidade de São Paulo
Instituto de Astronomia, Geofísica e Ciências Atmosféricas

INSTITUTO DE ASTRONOMIA,
GEOFÍSICA E CIÊNCIAS
ATMOSFÉRICAS

Introduction

The Pantanal wetland (Figure 1) is a Quaternary basin in Southwestern Brazil, reaching up to ~ 500 m of sedimentary package. Although the relatively recent formation of the basin, the mechanisms involved in the origin of the regional subsidence are not fully understood. Previous works proposed a flexural origin for the basin, invoking the last pulse of Andean tectonism and consequent topographic load as the source for the creation of the Pantanal Basin. However, taking into account the flexural rigidity of the South American lithosphere and the Andean geometry, it is difficult to explain the subsidence amplitude as well as the position of the basin due to flexural effects. Therefore, probably another mechanism must be involved in the formation and evolution of this active sedimentary basin.

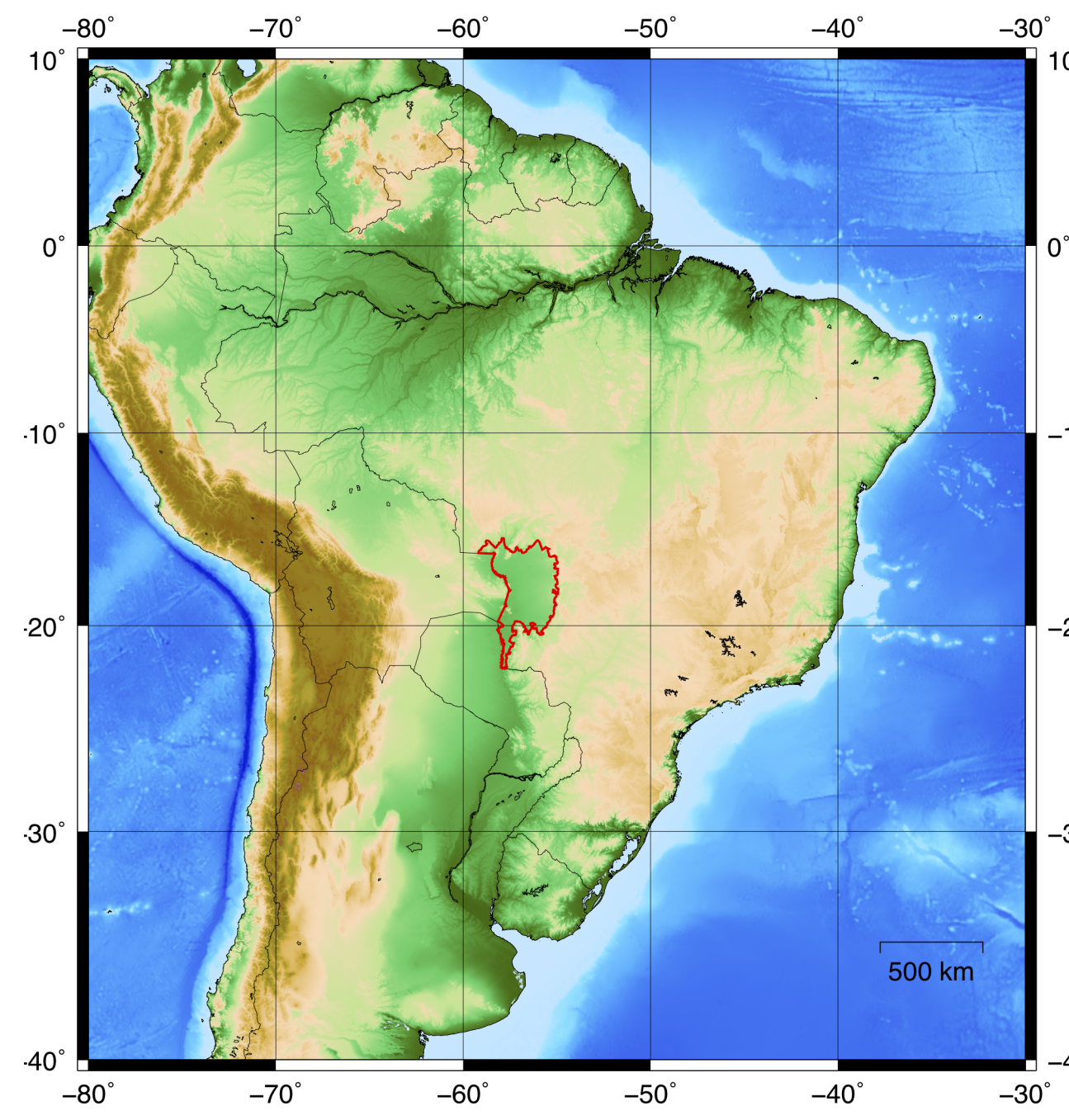


Figure 1: Map of South America showing the Pantanal Basin perimeter.

In the present work we will perform several 2D numerical simulations to evaluate how initial conditions can contribute to the buoyancy of the subducting Nazca plate. The results will be used in an upcoming study to calculate the influence of mantle convection generated by the subducting slab geometry and assess if it can induce dynamic topography and contribute to create the depression associated with the Pantanal Basin.

We used a finite element code to simulate the thermochemical convection in the mantle, calculating the associated dip angle of subduction along a profile from 80.0°W to 48.5°W , crossing the Pantanal wetland at a latitude of 18°S . To simulate the mantle flow, the thickness of both lithosphere and crust were resampled from the global LITHO1.0 model and the initial thermal structure for subducting slab was constructed based on a simplified thermokinematic model. The subducting slab geometry adopted was derived from the Slab2 model. The results will be considered to three dimensional models in the future to better represent latitudinal variations of the subducting slab and consequently improve the representation of the dynamic topography in the interior of the South American Plate.

Numerical Methods

We used the 3D finite element numerical code MD3D [5] to solve the Stokes flow for a fluid using the Boussinesq approximation in a Cartesian coordinate system. This resulted in the equations for conservation of mass (Equation 1), momentum (Equation 2) and energy (Equation 3) [8].

$$u_{i,i} = 0 \quad (1)$$

$$\sigma_{ij,j} + g\alpha\rho_0 T \delta_{ij} = 0 \quad (2)$$

$$\frac{\partial T}{\partial t} + u_i T_{,i} = \kappa T_{,ii} \quad (3)$$

where u_i is the velocity in the i direction, σ_{ij} is the stress tensor (Equation 4), g is the acceleration of gravity, ρ_0 is the mantle reference viscosity, α is the coefficient of thermal expansivity, T is temperature, δ_{ij} is the Kroenecker delta function, t is time, and κ is the thermal diffusivity.

$$\sigma_{ij,j} = -P\delta_{ij} + \eta(u_{i,j} + u_{j,i}) \quad (4)$$

where P is the dynamic pressure, and η is the viscosity.

Initial conditions

To study how the buoyancy changes as a function of the initial parameters, the length of the subducting oceanic lithosphere will be reduced to match the depth of 450 km and we will simulate for 5 Myr until it "recovers its original length. This will serve as well to allow flow beneath the subducting plate, restricted to the longitudinal direction.

Layer model

The chosen layer model for the simulations is a combination of the Slab2 model [2] and the LITHO1.0 model [4] (Figure 2). While the Slab2 provides data for the geometry of the subducting slab, the LITHO1.0 provides information about the thickness of the crust and the depth of the lithosphere-asthenosphere boundary (LAB).

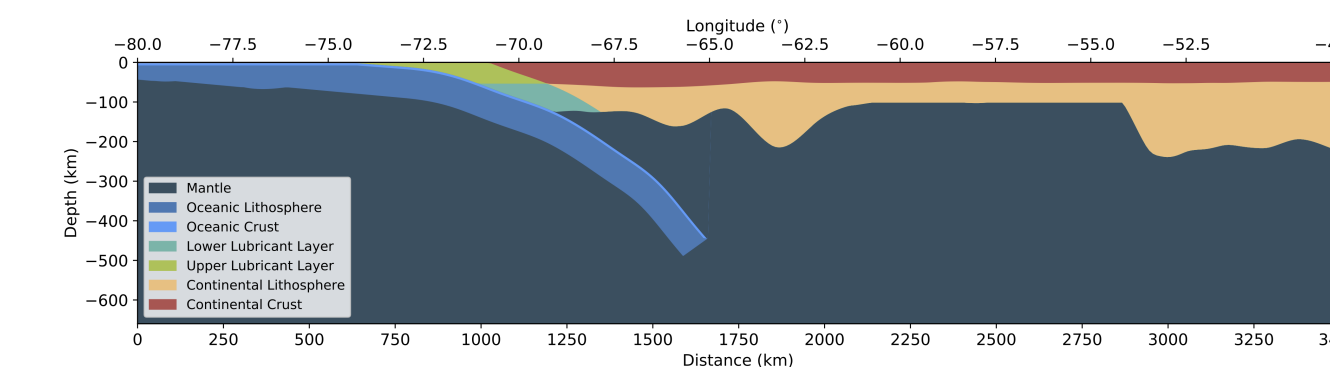


Figure 2: Example of an initial layer model with minimum LAB depth of 100 km in the continental regions and maximum oceanic crust depth of 7 km.

Thermal structure

The lithosphere temperature is assumed to increase with depth for both continental and oceanic regions. It starts at 0°C at the surface and increases linearly until 1300°C at the bottom of the lithosphere. For the asthenosphere, the geothermal gradient respects the adiabatic relation shown in Equation 5.

$$T(z) = (T_0 - 273.15) \exp \frac{\alpha g z}{C_p} \quad (5)$$

where T_0 is the potential temperature of the mantle on the surface, $\alpha = 3.28 \cdot 10^{-5} \text{ K}^{-1}$ is the thermal expansion coefficient, $g = 9.8 \text{ m/s}^2$ is the gravity acceleration, and $C_p = 1250 \text{ J/K s}^2$ is the heat capacity. T_0 is defined such that the temperature on the bottom of the model is 1518.68°C . This value is chosen to make the viscosity at that depth equals to 10^{19} Pa s .

For the subducting oceanic slab, we consider a semi-infinite slab of velocity v descending into an isothermal mantle and solved Equation 3 for $\partial T/\partial t = 0$. Furthermore, we added a contribution $\delta T = T(z) - T_0$, which is the difference between the potential temperature of the mantle on the surface and the temperature $T(z)$ at a certain depth z .

To simulate the heat conduction during before the simulation, we diffused the thermal structure for 20 Myr using the boundary condition of $\partial T/\partial x = 0$ on the sides of the model.

Velocity field

The imposed velocity field does not allow normal velocities on the bottom and on the surface of the model. On the sides, the velocity is chosen to cause the oceanic lithosphere to move with velocity v towards the continent. In the asthenosphere, this velocity decreases to zero with the error function. Because of Equation 1, a velocity field is defined to the other side of the model, but with maximum velocity at the bottom, decreasing to zero with the error function and being null for the continental lithosphere.

A velocity field was also defined for the surface of the model, where the velocity of the oceanic lithosphere was set to be constant and equal to the normal velocity v . For the continental lithosphere, we set the velocity to be zero, as the subducting slab should move relative to it. Because the slab would anchor in the continental lithosphere during the subduction, we also set a constant velocity v for the first 200 km of the continental lithosphere. Although this distance seems big, the dip angle of the subducting slab is small.

Initial conditions - continuation

Rheology model

The viscosity will be considered to vary exponentially as a function of the temperature T and a compositional factor C as in the Frank-Kamenetski approximation (Equation 6). We consider the mantle to be a fluid of variable viscosity for a steady state ductile creep, as it is usually considered for thermochemical convection [6].

$$\eta(T, C) = C \eta_r b^* \exp(-\gamma T) \quad (6)$$

where η_r is the reference viscosity, b^* and $\gamma = E_a/RT_b^2$ are constants and where E_a is the activation energy, R is the gas constant, and T_b is the basal temperature.

Results

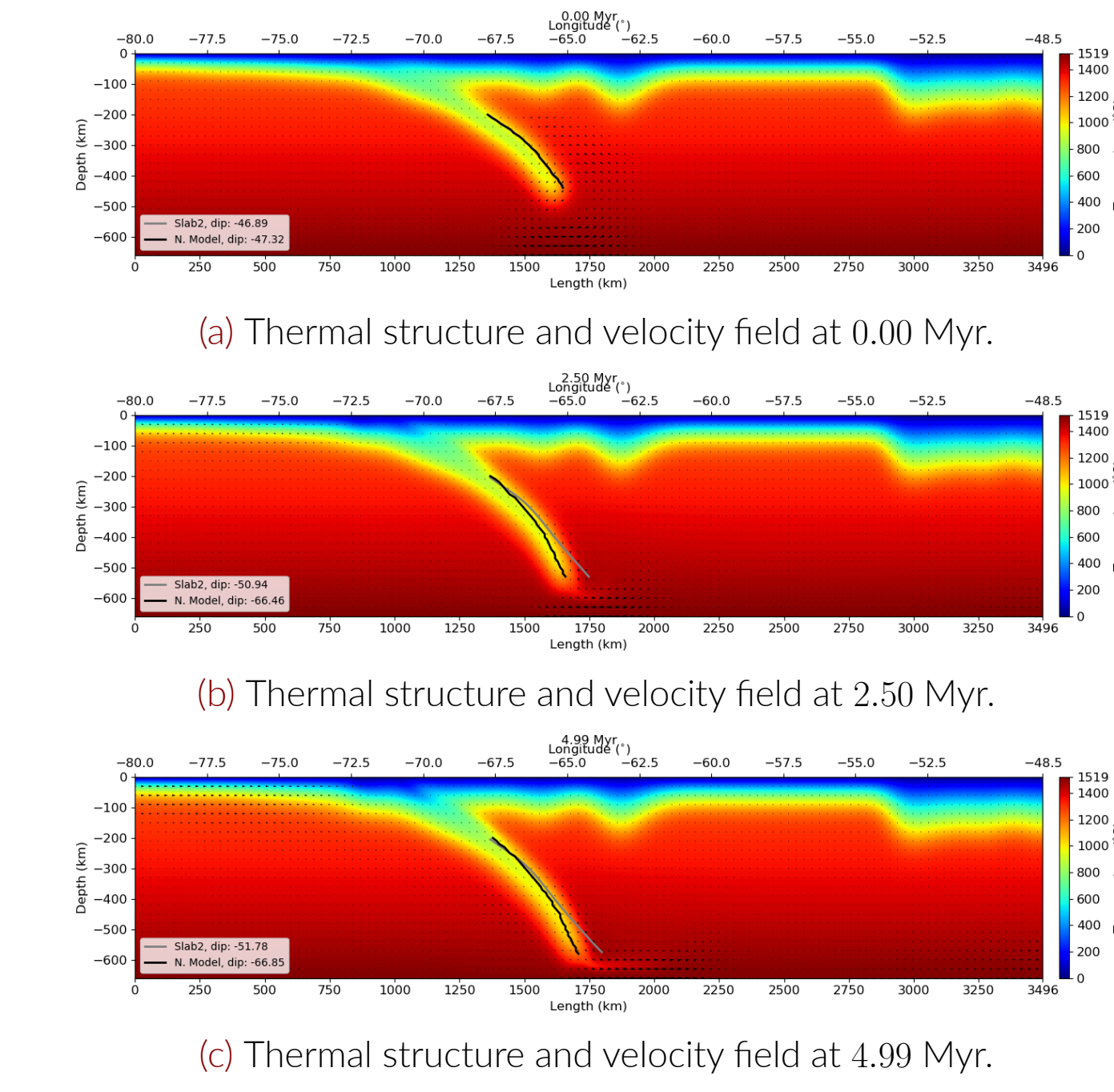


Figure 3: Temperature and velocity profiles showing the evolution of the dip angle of the subducting slab until 4.99 Myr. The simulation was made using a thicknesses of 85 km for the subducting slab, and 6 km for the oceanic crust. The compositional factors are $C = 1000$ for the lithosphere, $C = 1$ for the mantle, and $C = 0.01$ for the lubricant layer. Densities are $\rho_m = 3300 \text{ kg/m}^3$ for the mantle, $\rho_{cc} = 2750 \text{ kg/m}^3$ for the continental crust, and $\rho_{oc} = 2800 \text{ kg/m}^3$ for the oceanic crust.

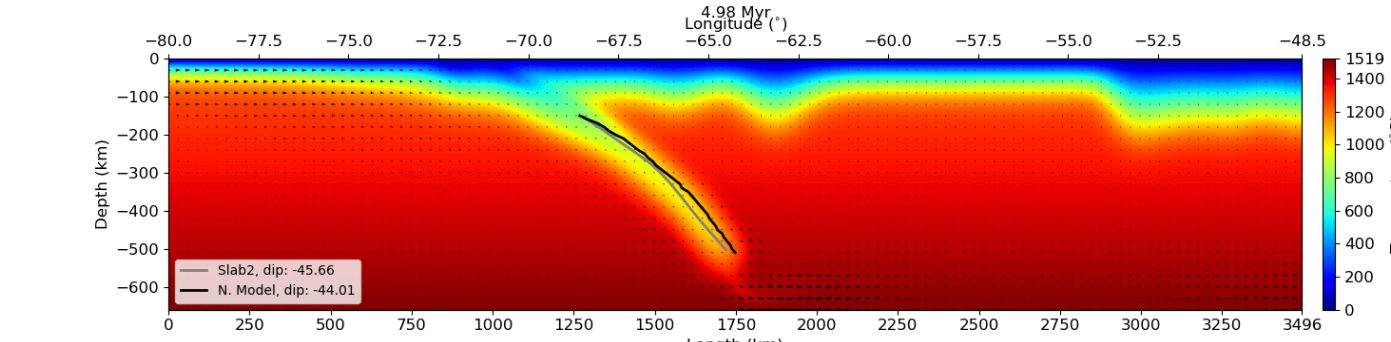


Figure 4: Simulation with the smallest dip angle difference between the Slab2 and the simulation at 4.98 Myr. The thicknesses of the subducting slab and the oceanic crust are 80 and 7 km, respectively. The compositional factors are $C = 1000$ for the lithosphere, $C = 1$ for the mantle, and $C = 0.01$ for the lubricant layer. Densities are $\rho_m = 3300 \text{ kg/m}^3$ for the mantle, $\rho_{cc} = 2750 \text{ kg/m}^3$ for the continental crust, and $\rho_{oc} = 2800 \text{ kg/m}^3$ for the oceanic crust.

Conclusions

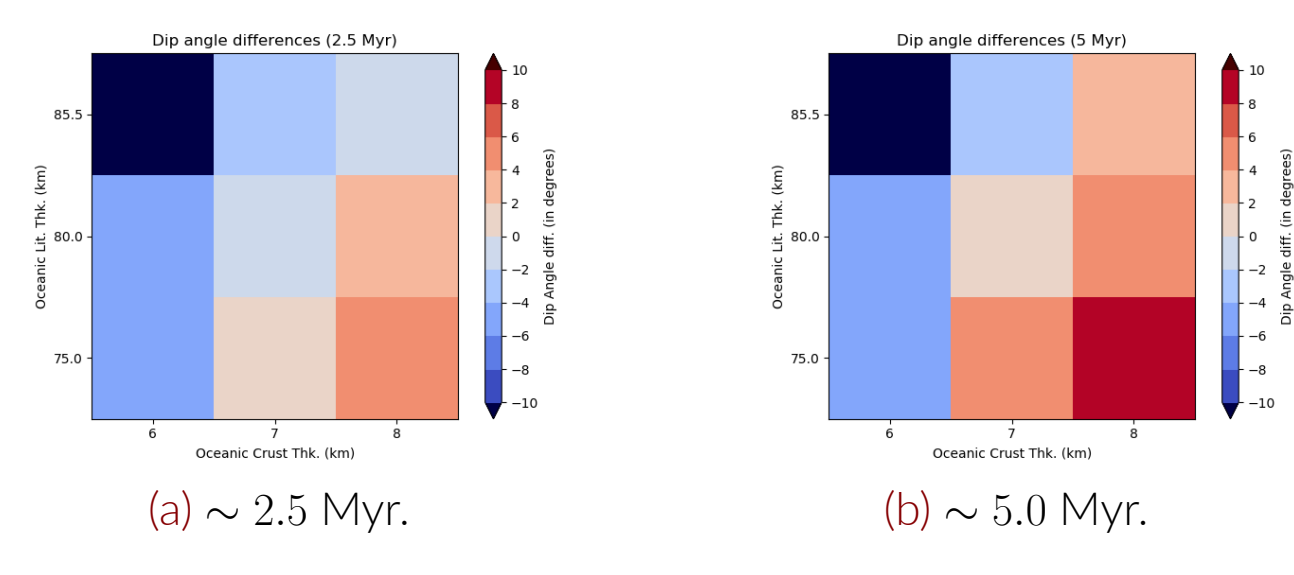


Figure 5: Results for a few combinations of oceanic lithosphere thickness and oceanic crust thickness showing the difference between the dip angles of the simulated subducting slab and the Slab2 model. The difference was calculated at two distinct steps for each simulation.

Next Steps

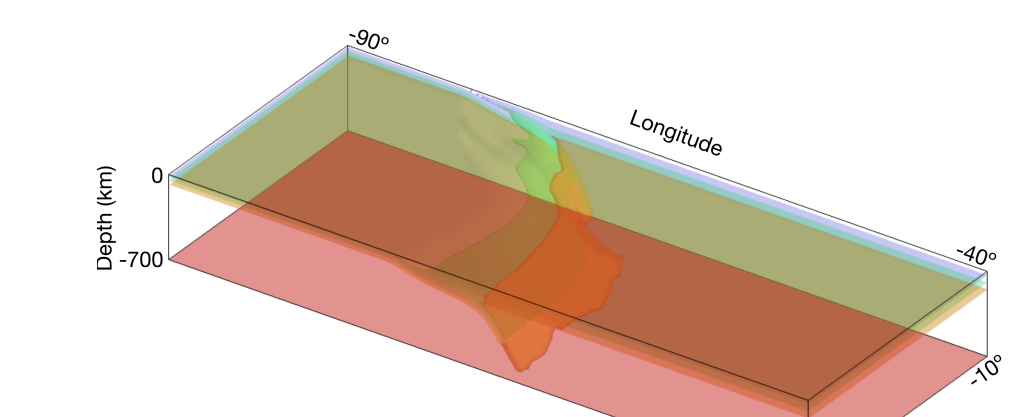


Figure 6: Initial thermal structure for a 3D grid.

References

- [1] Marcelo Assumpção and Gerardo Suárez.
Source mechanisms of moderate-size earthquakes and stress orientation in mid-plate